Applied Surface Science 257 (2011) 8784–8787

Contents lists available at ScienceDirect

Applied Surface Science

journal homepage: www.elsevier.com/locate/apsusc

Improving the photoluminescence properties of self-assembled InAs surface quantum dots by incorporation of antimony

C.H. Chiang[a,*], Y.H. Wu[b], M.C. Hsieh[a], C.H. Yang[a], J.F. Wang[a], Ross C.C. Chen[a], L. Chang[b], J.F. Chen[a]

[a] Department of Electrophysics, National Chiao Tung University, Hsinchu, Taiwan, ROC
[b] Department of Materials Science and Engineering, National Chiao Tung University, 1001, Ta-Hsueh Rd., Hsinchu, Taiwan, ROC

ARTICLE INFO

Article history:
Received 19 January 2011
Received in revised form 31 March 2011
Accepted 1 April 2011
Available online 27 May 2011

Keywords:
InAs
Surface quantum dot
Antimony
Surfactant
Segregation

ABSTRACT

This study investigates the effects of surfactant and segregation from InAs surface quantum dots (SQDs) by incorporating antimony (Sb) into the QD layers. The Sb surfactant effect extends planar growth and suppresses dot formation. Incorporating Sb can reduce the density of SQDs by more than two orders of magnitude. Photoluminescence (PL) reveals enhancement in the optical properties of InAs SQDs as the Sb beam equivalent pressure (BEP) increases. This improvement is caused by the segregation of Sb on the surface of SQDs, which reduces non-radiative recombination and suppresses carrier loss. The dark line at the SQDs surface in the transmission electron microscopic image suggests that the incorporated Sb probably segregates close to the surface of the SQDs. These results indicate a marked Sb segregation effect that can be exploited to improve the surface-sensitive properties of SQDs for biological sensing.

1. Introduction

Self-assembled InAs quantum dots (QDs) [1–5] are of great interest because of their practical applications and usefulness in scientific studies. Motivated by the advantages of incorporating antimony (Sb) as a surfactant into a strained InGaAs quantum well (QW) to delay three-dimensional (3D) growth and thus to extend the emission wavelength by reducing the surface faceting and delaying the formation of dislocations, several studies have investigated the incorporation of Sb [6–9] or bismuth [10] in InAs or InGaAs QDs. Sb has received a great deal of attention owing to its surfactant properties. Surfactant species segregate to the growth front and decrease surface energy and surface diffusion, offering another means of controlling the growth of QDs [11]. Dilute Sb that is incorporated into InAs buried quantum dots (BQDs) has been demonstrated to emit at 1.3 μm at room temperature [12]. Matsuura et al. observed that the incorporation of Sb into InGaAs QDs reduced the density of surface quantum dots (SQDs) [13] and attributed this decrease to an Sb surfactant effect, which extends planar growth and suppress dot formation. Recent years have seen tremendous interest in the properties of uncapped In(Ga)As QDs (SQDs), owing to their potential biological sensing applications [14,15], which exploit their surface-sensitive properties [16–19]. However, the range of applications of SQDs is limited by the fact that their PL performance is worse than that of BQDs. Liang et al. observed that the optical performance of SQDs can be improved by controlling the number of stacked QD layers or the thickness of GaAs spacers [20]. The purpose of this research is to improve the PL properties of InAs SQDs by directly incorporating various amounts of Sb, and to characterize their optical and structural properties. The Sb segregation effect in InAsSb SQDs is also studied using transmission electron microscopy (TEM).

2. Experimental

InAsSb QDs were grown on n^+-GaAs (1 0 0) substrates by molecular beam epitaxy in a Riber Epineat machine. A 0.3 μm-thick Si-doped GaAs buffer layer (3×10^{16} cm^{-3}) was initially grown at 595 °C at a growth rate of 3.03 Å/s. Then, the growth temperature was lowered to 485 °C to grow QDs at a growth rate of 0.256 Å/s by depositing a 2.72 ML-thick InAs(Sb) layer. Four samples were grown with Sb beam equivalent pressures (BEPs) of 0, 1.4×10^{-8}, 1.8×10^{-8}, and 6×10^{-8} Torr, respectively. The beams were supplied from an Sb cracker. Then, the QDs were capped with a 50 Å-thick $In_{0.15}Ga_{0.85}As$ layer, which was grown at 485 °C at a rate of 1.88 Å/s and a 0.3 μm-thick Si-doped GaAs top layer (3×10^{16} cm^{-3}), which was grown at 595 °C. To analyze accurately the effect of Sb segregation, similar QDs without a cap layer were also grown on the surface of the sample. Details of the growth of the QDs have been presented elsewhere [21]. Photoluminescence (PL) measurements were made using a double-frequency

* Corresponding author.
E-mail address: ziglar0316@gmail.com (C.H. Chiang).

0169-4332/$ – see front matter.
doi:10.1016/j.apsusc.2011.04.006

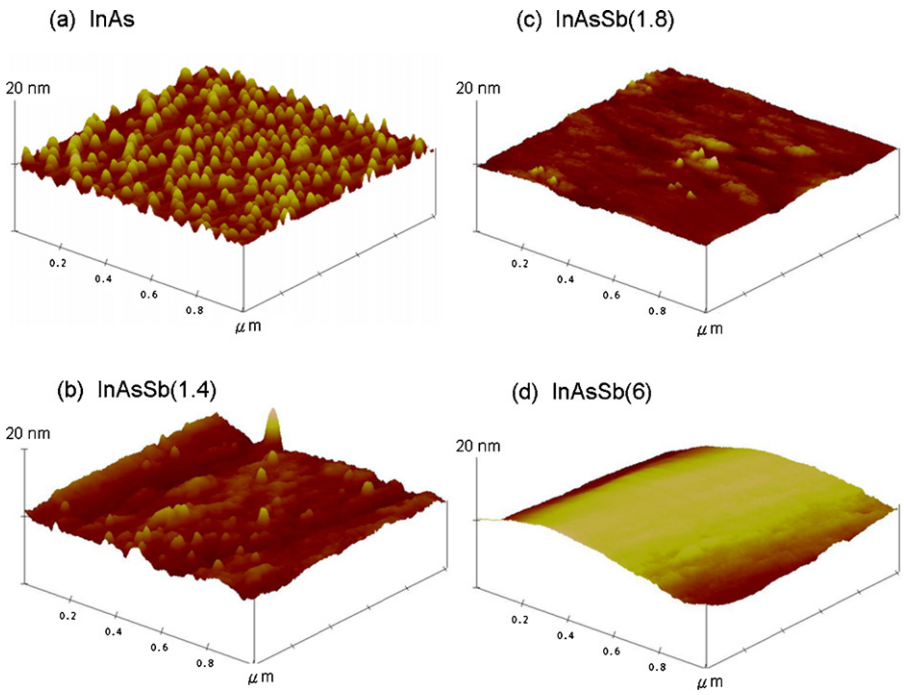

Fig. 1. $1 \times 1\ \mu m^2$ AFM three-dimensional images of 2.72 ML InAs(Sb) surface QDs, deposited on surface of sample under Sb BEPs of (a) 0, (b) 1.4×10^{-8}, (c) 1.4×10^{-8},and (d) 6×10^{-8} Torr. Sb incorporation reduces dot density by more than two orders of magnitude.

Nd-doped yttrium-aluminum-garnet (YAG) laser with a wavelength of 532 nm. Atomic force microscopy (AFM) measurements of the SQDs samples were made using a NanoScope III-a AFM from Digital Instrument. Specimens for cross-sectional TEM examination were prepared along the [1 1 0] GaAs direction by conventional polishing and gridding. Then, a low-voltage Ar ion miller was used to thin the specimen to a thickness of less than 50 nm for high-resolution TEM (HRTEM). The SQDs were characterized using a JEOL 2010F that was operated at 200 kV.

3. Results and discussion

Fig. 1(a)–(d) shows the three-dimensional AFM images ($1 \times 1\ \mu m^2$) of the InAs(Sb) SQDs at various Sb BEPs of (a) 0, (b) 1.4×10^{-8}, (c) 1.8×10^{-8} and (d) 6×10^{-8} Torr, respectively. [They are denoted InAs, InAsSb(1.4), InAsSb(1.8),and InAsSb(6), respectively.] Without Sb, the QD density was approximately $3 \times 10^{10}\ cm^{-2}$. Sample InAsSb(1.4) had a lower QD density of $3.5 \times 10^{9}\ cm^{-2}$, and sample InAsSb(1.8) had an even lower QD density of $6 \times 10^{8}\ cm^{-2}$. Incorporating Sb reduced the density of the SQDs by more than two orders of magnitude. These results are consistent with those of Matsuura et al. [13]. An Sb surfactant effect that can extend two-dimensional growth and suppress dot formation is responsible for this drop in dot density. Further increasing the Sb BEP to 6×10^{-8} Torr modifies the surface morphology to one of ellipsoid terraces of height ~9 nm, length ~4.5 μm, and width ~1.3 μm, as previously observed [22], indicating that the incorporated Sb acts as a surfactant and encourages 2D growth, as discussed with reference to highly strained InGaAs QWs [9]. A large Sb BEP worsens the surface morphology as a significant amount of the deposited material tends to form these thick terraces, rather than a thin wetting layer, as shown in Fig. 2. A few large islands are observed on top of these terraces. The dot density is too low to be determined accurately by AFM. However, since the AFM picture shows less than one dot in an area of $1 \times 1\ \mu m^2$, the estimated density is less than $1 \times 10^{8}\ cm^{-2}$. Cross-sectional TEM reveals a typical dot with a height of about 8.5 nm and a diameter of 27 nm. The density reduction is accompanied by size and shape modifications. The AFM results indicate that the Sb-free SQDs have an average lateral diameter of 50 nm and a height of 10 nm. In the sample InAsSb(1.4), the height is reduced to ~5 nm without significantly affecting the lateral diameter. In the sample InAsSb(1.8), the lateral diameter and height are reduced to 35 and 3 nm, respectively. Further increasing Sb BEP to 6×10^{-8} Torr yields a regular periodic surface morphology of ellipsoid terraces, as shown in Fig. 2. This reduction in dot size is consistent with the suppression of growth of the QDs by the surfactant and thus the Sb surfactant effect markedly affects the growth of the SQDs.

Fig. 3 shows the room-temperature PL spectra of samples InAs, InAsSb(1.4), InAsSb(1.8), and InAsSb(6). Each spectrum includes two groups of peaks. The peaks at ~0.77 eV are associated with the SQDs, and the peaks at 0.95–1.05 eV are associated with the BQDs. The BQD spectra include a doublet feature that is similar to the ground and first-excited transitions. The peaks at ~1.02 eV were confirmed to be caused by the electronic transition from the first-excited state of BQDs, as revealed by band-filling in the power-dependent PL measurement. Moreover, the energy separation between the ground-state PL peaks and the first-excited state PL peaks of the four samples is 73–75 meV, which is con-

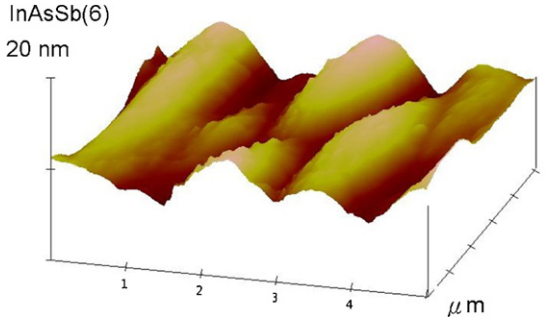

Fig. 2. Following Sb incorporation at a high Sb BEP of 6×10^{-8} Torr, a few larger islands are observed on top of ellipsoid terraces.

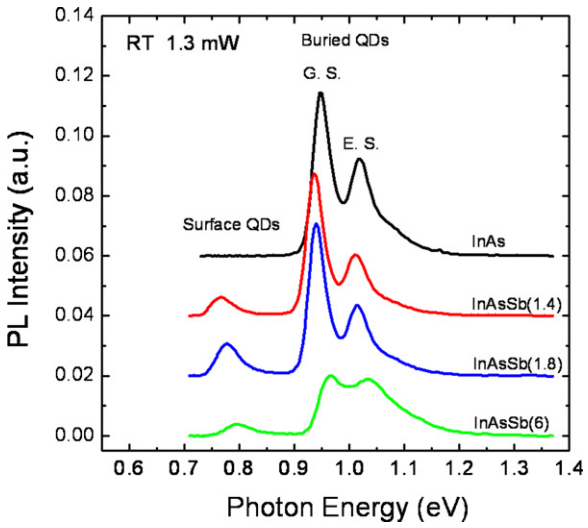

Fig. 3. Room-temperature PL spectra of samples obtained at an excitation power of 1.3 mW. Each spectrum includes two groups of peaks: those at ~0.77 eV are associated with surface QDs and those at ~0.95 eV are associated with buried QDs.

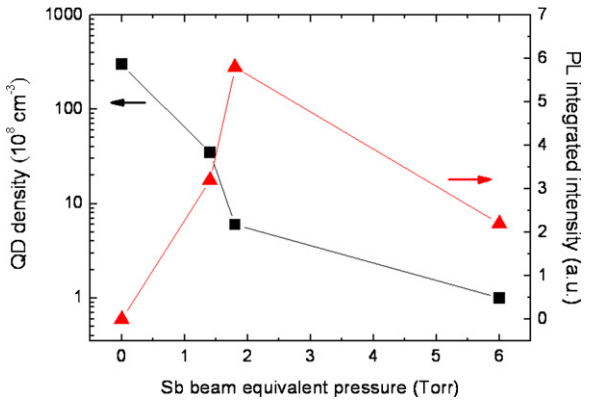

Fig. 4. Dot density (left axis) and integrated PL intensity (right axis) of InAs(Sb) surface QDs versus Sb beam equivalent pressure.

sistent with the values in previous reports [23]. Remarkably, the spectrum of InAsSb(1.4) includes a long-wavelength emission peak from SQDs around 0.765 eV (1620 nm) with a full width at half maximum (FWHM) of 40.93 meV, and a PL emission peak from BQDs centered around 0.936 eV with an FWHM of 30 meV. This result demonstrates that incorporating Sb into an InAs sample substantially improves the intensity of PL from the SQDs. When the QDs are covered by a 0.3 μm-thick GaAs cap layer, the emission from the BQDs is blue-shifted by about 171 meV; this shift is expected because of the change in strain as the band gap is increased with the growth of the GaAs capping layer [16–18]. The InAsSb/InGaAs QDs, capped by 0.3 μm-thick GaAs will tend to force the lattice constant back to that of the InGaAs, which is probably perfectly strained on GaAs, and the resulting BQDs are more strained than the SQDs. Miao et al. estimated a change in the energy gap of InAs QDs of about 195 meV in response to strain relaxation when the GaAs capping layer was removed [17]. Capping the QD with an InGaAs layer has been shown to reduce the strain and extend the range of emission wavelengths [24]. This strain-reducing InGaAs layer is expected to influence the change in the energy gap that is caused by the growth of the GaAs capping layer. The spectrum of InAsSb(1.8) also includes a long-wavelength emission peak around 0.775 eV from SQDs, with an FWHM of 42.23 meV. Notably, the PL intensity increases as the Sb BEP is increased further. Sample InAsSb(1.8) yields the highest PL intensity, which at 300 K, is approximately 4.5 times less than that of BQDs. This result differs importantly from that in the literature [17,19], in which it is approximately one to two orders of magnitude lower than that of BQDs – a result obtained using no Sb in the growth process. Therefore, the PL intensity of the SQDs is much lower, which result is expected owing to the increase in the non-radiative recombination of electron–hole pairs via surface states [17]. In this study, the transfer of carriers from the BQDs to the SQDs may not be responsible for the improvement [20], because a 0.3 μm-thick GaAs blocking layer separates the BQDs from the SQDs. Rather, the enhancement is believed to be strongly related to the incorporation of Sb into the QD layers. The emission from the SQDs is blue-shifted from 0.765 to 0.795 meV as Sb BEP increases. This blue-shift is attributed to a reduction in the dot height by the Sb surfactant effect. However, the FWHM of the PL spectral peak herein is 40–50 meV, which differs considerably from the corresponding result in the literature [17,19], in which the smallest PL linewidth for SQDs is about 100 meV. This difference is explained by the uniformity of the sizes and surface of the SQDs for which the Sb surfactant effect is responsible. These results show that the incorporation of Sb effectively improves the PL performance of InAs SQDs. The literature has shown that In segregation at the surface of InGaAs SQDs increases PL intensity even at room temperature, by suppressing non-radiative surface recombination [16]. The data herein further support the claim that the PL intensity of SQDs is enhanced by the same mechanism. The optical behavior of SQDs is very poor owing to surface states, as evidenced by their weak and broad PL [20]. The surface states arose from the dangling bonds in the SQDs [17]. The tunneling of excitons from the confined quantum states of the SQDs to the surface states causes the intensity of PL from the SQDs to be typically quite weak [25]. This weakness arises from the reduction of radiative recombination as the number of carriers that tunnel to the surface states, in which non-radiative recombination occurs, increases. The recombination velocities at the GaAs and InAs surfaces are about 10^6 and 10^4 cm/s respectively, and so the carriers vanish at these surfaces [16]. However, InSb has a lower surface recombination velocity of around 10^3 cm/s [26], indicating lower carrier loss at its surface. Accordingly, the enhancement of PL from InAs SQDs indicates the abundance of Sb close to the surface, and that the surface of the dots is almost entirely InSb because Sb is segregated.

Fig. 4 plots the density of QDs (left axis) and the PL integrated intensity (right axis) of the InAs SQDs versus the Sb BEP. The integrated PL intensity increases considerably with the Sb BEP from 0 to 1.8×10^{-8} Torr. However, it decreases as the Sb BEP is increased further. This phenomenon can be interpreted as reflecting a change of SQD density, as shown in Fig. 4 (left axis). The AFM measurements reveal that the incorporation of Sb effectively reduces the density of the SQDs by an Sb surfactant effect, which enhances layer-by-layer growth and suppresses dot formation. In particular, the incorporation of Sb from a BEP of 0 to a BEP of 1.8×10^{-8} Torr reduced the density of the SQDs by more then one order of magnitude, but the integrated PL intensity of the SQDs still increased. To confirm that the segregation of Sb can improve the PL of InAs SQDs, a further investigation must be performed to identify Sb segregation close to the surface of SQDs. Fig. 5(a) and (b) show cross-sectional TEM images of sample InAsSb(1.4) and sample InAsSb(6), respectively. Based on the images projected along the [1 1 0] GaAs direction, the SQDs in these two samples are pyramidal with a contact angle of ~27.7°. Obviously, increasing the Sb BEP reduces the dot density and the slightly roughens of the surface. In Fig. 5(b), the surface exhibits a characteristic angle of ~174°. A few large islands are observed on top of the terrace. We suggest that the large islands exhibit no 3D quantum confinement. Their diameter (~100 nm, ≫de Brogli wavelength) is too large to modify the confinement energy efficiently. The TEM image of InAsSb(6) clearly proves the

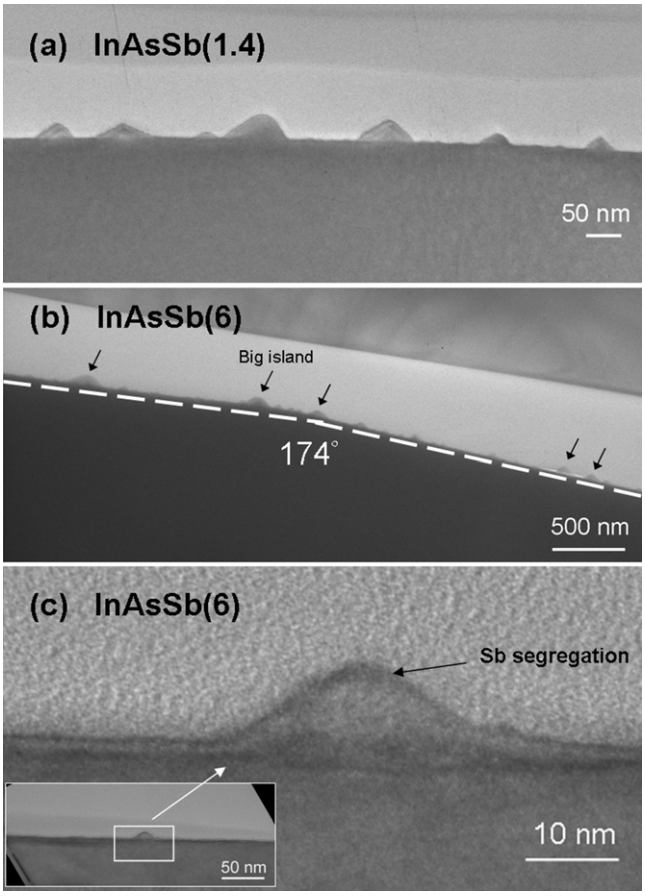

Fig. 5. Cross-sectional TEM images of (a) sample InAsSb(1.4) and (b) sample InAsSb(6). (c) HRTEM image of InAsSb(6) surface QD; inset shows the same area at low magnification: Sb segregation close to the surface is clearly observed.

PL peak around 0.79 eV from SQDs, even when the dot density is reduced to $\sim 1 \times 10^8$ cm^{-2}. Fig. 5(c) shows an HRTEM image of InAsSb(6) SQDs and the inset shows the same area at a low magnification. The dot is a full pyramidal with a base diagonal of 27 nm and a height of 8.5 nm. The dark line at the dot surface probably reveals segregation of the heavy element at the surface. Similar results are also observed from other SQDs in samples InAsSb(6) and InAsSb(1.4). The segregation of Sb provides a Sb-rich surface coverage, and promotes the surfactant effect. This surfactant effect is related to thermodynamics (associated with a change of the surface free energy of the growing film) or kinetics (associated with a reduction of the surface diffusion of adatoms). Harmand et al. observed that Sb is not easily incorporated into highly strained InGaAs on GaAs when it is supplied during its growth [7]. InAsSb SQDs have a lattice constant that is larger than that of GaAs, and the strain relaxation is largest at the top of the QDs [17]. In this study, strong compressive stress was induced at the bottom of the SQDs and weak compressive stress was present at the surface of the SQDs. The bottom of the SQDs is strained to match the GaAs substrate, while the top of the SQDs is relaxed according to the intrinsic lattice constant of InAsSb. As a result, a continuous strain distribution is established in the SQDs. Therefore, the lens-shaped darker area at the bottom of the pyramidal structure is the region of higher compressive strain at the bottom of the SQD, as shown in Fig. 5(C). This effect is a consequence of the higher compressive strain at the bottom of the SQDs, which inhibits the incorporation of the large Sb atoms. Accordingly, the growth proceeds with strong Sb surface segregation, which alters the reconstruction of the surface, as observed by *in situ* reflection high-energy electron diffraction during the growth. As previously mentioned, the HRTEM images reveal Sb segregation close to the surface, indicating that Sb passivation on the surface of the SQDs increased the PL intensity, inhibiting the non-radiative recombination and suppressing carrier loss at the SQDs.

4. Conclusions

In conclusion, surfactant and segregation effects of Sb in InAs(Sb) SQDs were investigated. The Sb surfactant effect can extend planar growth and suppress dot formation. The findings in this study suggest that the PL of InAsSb SQDs is strengthened by increasing Sb BEP. The enhancement of the integrated intensity of PL is attributable to Sb segregation close to the surface of SQDs, and reduces non-radiative recombination. The dark line at the surface of the SQDs in the TEM image suggests that the incorporated Sb probably segregates close to the surface of the SQDs. The segregation of Sb provides a Sb-rich surface coverage, and promotes the surfactant effect. This research opens up an interesting avenue for investigating the possibility of using InAs(Sb) SQDs as biological markers and sensors.

Acknowledgments

The authors would like to thank the National Science Council of the Republic of China, Taiwan (contract No. NSC-97-2112-M-009-014-MY3) and the Ministry of Education of the Republic of China, Taiwan, under the ATU program for financially supporting this research. Dr. J.Y. Chi and R.S. Hsiao are commended for preparing the samples.

References

[1] F. Heinrichsdorff, M.-H. Mao, N. Kirstaedter, A. Krost, D. Bimberg, Appl. Phys. Lett. 71 (1997) 22.
[2] D.J. Eaglesham, M. Cerullo, Phys. Rev. Lett. 64 (1990) 1943.
[3] S. Guha, A. Madhukar, K.C. Rajkumar, Appl. Phys. Lett. 57 (1990) 2110.
[4] C.W. Snyder, J.F. Mansfield, B.G. Orr, Phys. Rev. B 46 (1992) 9551.
[5] Y. Arakawa, H. Sakaki, Appl. Phys. Lett. 40 (1982) 939.
[6] T. Kageyama, T. Miyamoto, M. Ohta, T. Matsuura, Y. Matsui, T. Furuhata, F. Koyama, J. Appl. Phys. 96 (2004) 44.
[7] J.C. Harmand, L.H. Li, G. Patriarche, L. Travers, Appl. Phys. Lett. 84 (2004) 3981.
[8] X. Yang, M.J. Jurlovic, J.B. Heroux, W.I. Wang, Appl. Phys. Lett. 75 (1999) 178.
[9] H. Shimizu, K. Kumada, S. Uchiyama, A. Kasukawa, Electron. Lett. 36 (2000) 1379.
[10] B.N. Zvonkov, I.A. Karpovich, N.V. Baidus, D.O. Filatov, S.V. Morozov, Y.Y. Gushina, Nanotechnology 11 (2000) 221.
[11] D. Guimard, M. Ishida, L. Li, M. Nishioka, Y. Tanaka, H. Sudo, T. Yamamoto, H. Kondo, M. Sugawara, Y. Arakawa, Appl. Phys. Lett. 94 (2009) 103116.
[12] K. Suzuki, Y. Arakwa, Phys. Status Solidi B 224 (2001) 139.
[13] T. Matsuura, T. Miyamoto, T. Kageyama, M. Ohta, Y. Matsui, T. Furuhata, F. Koyama, Jpn. J. Appl. Phys. 43 (2004) L605.
[14] W.C. Chen, S. Nie, Science 281 (1998) 2016.
[15] A. Madhukar, S. Lu, A. Konkar, Y. Zhang, M. Ho, S.M. Huges, A.P. Alivisatos, Nano Lett. 5 (2005) 479.
[16] H. Saito, K. Nishi, S. Sugou, Appl. Phys. Lett. 73 (1998) 2742.
[17] Z.L. Miao, Y.W. Zhang, S.J. Chua, Y.H. Chy, P. Chen, S. Tripathy, Appl. Phys. Lett. 86 (2005) 031914.
[18] Y. Ziad, E. AbuWaar, Jr. Marega, M. Mortazavi, G.J. Salamo, Nanotechnology 19 (2008) 335712.
[19] Z.F. Wei, S.J. Xu, R.F. Duan, Q. Li, J. Wang, Y.P. Zheng, H.C. Liu, J. Appl. Phys. 98 (2005) 084305.
[20] B.L. Liang, Zh.M. Wang, Yu.I. Mazur, G.J. Salamo, A. Eric, Jr. DeCuir, M.O. Manasreh, Appl. Phys. Lett. 89 (2006) 043125.
[21] J.F. Chen, R.S. Hsiao, W.D. Huang, Y.H. Wu, L. Chang, J.S. Wang, J.Y. Chi, Appl. Phys. Lett. 88 (2006) 233113.
[22] J.F. Chen, C.H. Chiang, Y.H. Wu, L. Chang, J.Y. Chi, J. Appl. Phys. 104 (2008) 023509.
[23] J.F. Chen, Y.Z. Wang, C.H. Chiang, R.S. Hsiao, Y.H. Wu, L. Chang, J.S. Wang, T.W. Chi, J.Y. Chi, Nanotechnology 18 (2007) 355401.
[24] J. Tatebayashi, M. Nishioka, Y. Arakawa, Appl. Phys. Lett. 78 (2001) 3469.
[25] B.L. Liang, Yu.I. Mazur, P. Vas, Zh. Kunets, M. Wang, G.J. Salamo, E.A. DeCuir Jr., B. Passmore, M.O. Manasreh, Nanotechnology 19 (2008) 065705.
[26] P.M. Nikolic, D.M. Todorovic, D.G. Vasiljevic, P. Mihajlovic, K. Radulovic, Z. Ristovski, J. Elazar, V. Blagojevic, M.D. Dramicanin, Microelectron. J. 27 (1996) 459–469 (6).